applied sciences

MDPI

Article

Photocatalytic Hydrogen Production from Glycerol Aqueous Solution Using Cu-Doped ZnO under Visible Light Irradiation

Vincenzo Vaiano and Giuseppina Iervolino *

Department of Industrial Engineering, University of Salerno, via Giovanni Paolo II, 132, 84084 Fisciano (SA), Italy
* Correspondence: giiervolino@unisa.it; Tel.: +39-089-96-4006

Received: 17 May 2019; Accepted: 24 June 2019; Published: 6 July 2019

Abstract: Cu-doped ZnO photocatalysts at different Cu loadings were prepared by a precipitation method. The presence of Cu in the ZnO crystal lattice led to significant enhancement in photocatalytic activity for H_2 production from an aqueous glycerol solution under visible light irradiation. The best Cu loading was found to be 1.08 mol %, which allowed achieving hydrogen production equal to 2600 μmol/L with an aqueous glycerol solution at 5 wt % initial concentration, the photocatalyst dosage equal to 1.5 g/L, and at the spontaneous pH of the solution (pH = 6). The hydrogen production rate was increased to about 4770 μmol/L by increasing the initial glycerol concentration up to 10 wt %. The obtained results evidenced that the optimized Cu-doped ZnO could be considered a suitable visible-light-active photocatalyst to be used in photocatalytic hydrogen production without the presence of noble metals in sample formulation.

Keywords: photocatalysis; visible light; Cu-doped ZnO; hydrogen; glycerol

1. Introduction

Hydrogen production from water under sunlight is, nowadays, one of the most ecological and rational alternatives for obtaining an energy carrier. Hydrogen is a zero-carbon-emission fuel and it is expected to be an important energy source in the near future [1]. Actually, hydrogen is mainly produced by natural gas through the steam methane reforming process [2]. Unfortunately, this approach involves the use of fossil fuels and CO_2 production, and for this reason, it is not considered sustainable. So, attention is increasingly being paid to eco-sustainable processes that can be carried out in mild conditions (at room temperature and pressure) and without the use of fossil fuels. In recent years, the photocatalytic process for hydrogen production from water has attracted considerable interest [3–5]. In particular, by means of heterogeneous photocatalysis, hydrogen can be produced mainly by two processes: the direct splitting of water into H_2 and O_2 [6,7] or the photoreforming of organic compounds [8]. This latter process represents a very attractive method for the removal of organic pollutants in wastewaters with the simultaneous valorization of these substances [9–11]. Photocatalytic H_2 production from water using organic substances as sacrificial agents has been studied since the 1980s [12]. For this purpose, different organic compounds such as methanol [13], ethanol [14], sugar [13], glycerol [15], and lactic acid [16] have been used. In particular, the use of glycerol as a sacrificial agent for H_2 production via the photoreforming process has aroused great interest [17,18]. The reason for this is the huge production of glycerol, the content of which in by-product streams from the biodiesel industry is about 10 wt %, while glycerol itself still has limited demand in the market [19]. In the literature, there are several papers on the efficiency of photocatalysis for hydrogen production starting from a glycerol aqueous solution [18,20,21]. In particular, different photocatalysts have been tested and the most investigated ones were TiO_2-based materials [12,22]. However, the fast

recombination of photogenerated electron–hole pairs and the large band gap of semiconductors may hinder their photocatalytic performances. Forming composites with another semiconductor or adding metal nanoparticles represents an interesting strategy that has been developed to solve this problem. For example, photocatalytic systems, such as TiO_2–CuO_x, TiO_2–Pt, TiO_2–Pd, and NiO–TiO_2, have been studied for photocatalytic hydrogen production from a glycerol aqueous solution [21,23]. These synthesized photocatalysts proved to be much more active with respect TiO_2 alone, since the separation of the electron–hole pairs was improved. In addition, with the ZnO–ZnS/graphene composite, using a glycerol solution at 10 wt % initial concentration, the hydrogen production was equal to 289 µmol/L after 3 h of UV irradiation time [24]. Interesting results have also been reported for the Ag_2O/TiO_2 photocatalyst that, in the presence of glycerol and after 4 h of UV irradiation time, was able to produce 2100 µmol/L [25]. However, in order to use solar energy, the development of visible-light-driven photocatalytic systems is highly required. For this purpose, the use of a noble metal, such as Au, Ag, and Pt, as a cocatalyst element or for photocatalyst doping has been reported [26–28]. Generally, the effect of the presence of the noble metal is the plasmon resonance absorption property in the visible light region [29]. Specifically, the noble metal's roles are the enhancement of visible light absorption of the photocatalyst and the separation of photogenerated charges in semiconductors, such as TiO_2 or ZnO. For example, Pt/TiO_2 samples, under visible light and in the presence of glycerol (50 wt % initial concentration) and methanol, have produced about 7500 µmol/L of H_2 after 5 h of irradiation time, while in presence of only TiO_2, the hydrogen production was equal to only 500 µmol/L [30]. However, practical applications of photocatalytic hydrogen production based on a noble metal cocatalyst are restricted due to their high cost. So, as an alternative, it has been proposed to use different metals that are less expensive than noble metals but with interesting properties. This is the case with copper, which, as demonstrated in the literature [23,31,32], is able to enhance the photocatalytic properties of semiconductors such as TiO_2 and ZnO, promoting hydrogen production even in the presence of visible light. It has been reported that Cu nanoparticles, loaded on the TiO_2 surface by the photodeposition method, enhanced visible light absorption due to the plasmon resonance effect and also acted as cocatalysts to separate photogenerated charges in TiO_2 [33]. As a result, Cu/TiO_2 photocatalysts exhibited enhanced photocatalytic hydrogen production under visible light from a glycerol aqueous solution [33]. In this case, the maximum hydrogen production rate was equal to 0.24 mmol h^{-1} g^{-1}. However, an excessive addition of Cu decreased the hydrogen production rate, suggesting that copper nanoparticles on the TiO_2 surfaces hinder photon absorption [33]. Moreover, the role of copper as a cocatalyst or a doping element for semiconducting materials has been clarified in a recent review paper [34]. In particular, the review highlighted several papers concerning different species of copper used as cocatalysts for titanium dioxide [34]. The author showed that, generally, copper is present on the semiconductor surface, which in turn is coupled to another semiconductor such as graphene and alumina [35]. ZnO has recently generated much interest within the scientific community. In fact, this semiconductor is a promising material due to its environmental stability, low cost compared with other metal oxides [31], and good photocatalytic property [36,37]. ZnO has a band gap energy similar to TiO_2, being equal to 3.2 eV. As a consequence, it is active mainly in the presence of UV light [38]. In order to make it active under visible light irradiation, different strategies have been proposed in the literature for ZnO doping. Among these, the introduction of different types of metal dopant (e.g., Co, Mn, and Ni) into a ZnO semiconductor has been reported [39]. Different papers report the use of Cu-doped ZnO as an effective photocatalytic material [31,40]. However, this photocatalyst was studied mainly for the degradation of organic pollutants from water and wastewater [40–43]. In the recent years, the effect of Cu ions in ZnO nanorod arrays for photoelectrochemical water splitting under visible light was investigated [44]. In this work, the authors reported a considerable photocurrent density equal to 18 µA/cm^2 at 0.8 V during the water splitting reaction, which was about 11 times higher than that of undoped ZnO nanorod arrays. However, no data about the effective hydrogen production was reported. On the other hand, the use of Cu-doped ZnO as a photocatalyst for H_2 production from a glycerol aqueous solution has not been extensively investigated yet. For this reason, the aim of this

work was to evaluate the influence of operating conditions on photocatalytic hydrogen production from glycerol solutions in the presence of a visible-light-active Cu-doped ZnO photocatalyst, previously optimized towards the photocatalytic degradation of methylene blue and oxidation of arsenite into arsenate [37].

2. Experimental

2.1. Photocatalyst Preparation

The photocatalyst synthesis procedure was reported in our previous work [37]. ZnO and Cu-doped ZnO were synthesized by a simple precipitation method. In detail, 5 g of zinc acetate–dihydrate $ZnC_4H_6O_4$ (Aldrich Italy, 99%) was dissolved in 50 mL of distilled water. Once the zinc acetate had completely dissolved in water, a solution of NaOH, obtained by dissolving 2 g of NaOH in 25 mL of distilled water, was slowly added to the acetate solution in order to obtain a precipitate. In the case of Cu-doped ZnO, a specific amount of copper acetate hydrate $Cu(CH_3COO)_2$ was dissolved into the solution of $ZnC_4H_6O_4$ beforehand to induce the precipitation by NaOH addition. Finally, the generated precipitate was centrifuged, washed, and calcined at 600 °C for 2 h.

The Cu nominal loading is expressed as molar percentage and it was evaluated through the following relationship:

$$\%mol\ Cu = \frac{nCu}{nCu + nZn} \times 100$$

where:

nCu is the number of moles of $Cu(CH_3COO)_2$ used in the synthesis; and
nZn is the number of moles of $Zn(CH_3COO)_2\ 2H_2O$ used in the synthesis.

All the synthesized photocatalysts are listed in Table 1.

Table 1. List of the prepared samples with the nominal Cu loading and band gap energy.

Photocatalyst	Cu Nominal Amount (mol %)	Band Gap Energy (eV)
ZnO	data	3.19
0.54Cu_ZnO	0.54	3.02
1.08Cu_ZnO	1.08	2.92
2.15Cu_ZnO	2.15	2.94
4.21Cu_ZnO	4.21	2.91

These samples were well characterized in our previous work [37]. In particular, XRD analysis revealed the formation of ZnO with a hexagonal wurtzite structure for all the prepared samples. Moreover, with respect to undoped ZnO, a slight shift of XRD peaks towards a higher angle was observed for the Cu-doped ZnO photocatalysts (see Supplementary Materials, Figure S1). This phenomenon is due to the narrowing of the crystal lattice of ZnO, because Cu^{2+}, which has a cationic radius smaller than Zn^{2+}, can easily replace Zn^{2+} in the ZnO crystal lattice [45]. The morphology of the samples was evaluated by SEM analysis (see Supplementary Materials, Figure S2). From the SEM images, it was possible to note that the doping process did not change the overall morphology of the photocatalysts. In particular, both undoped ZnO and the 1.08Cu_ZnO photocatalyst were characterized by nonuniform macroaggregates.

The UV–Vis diffuse reflectance measurements evidenced that the Cu doping induced an improvement in the absorption of UV light and a decrease in the band gap value (Table 1), confirming that the Cu-doped photocatalysts can be activated by visible light, as evinced by the results of photocatalytic activity both in the degradation of methylene blue dye and in the oxidation of arsenite to arsenate [37].

2.2. Photocatalytic Activity Tests

The photocatalytic experiments for hydrogen production from glycerol aqueous matrices were carried out in a photocatalytic Pyrex cylindrical reactor (I D = 1.25 cm) equipped with a N_2 distributor device (Q = 0.122 NL/min) to assure the absence of O_2 during the tests. In a typical photocatalytic test, 0.0525 g of photocatalyst was suspended in 35 mL of a glycerol aqueous solution at 5 wt % of glycerol concentration. To ensure the complete mixing of the suspension in the reactor, a peristaltic pump was used. The photoreactor was irradiated with a strip of visible LEDs with the wavelength emission in the range of 400–600 nm (nominal power: 10 W; light intensity: 32 mW/cm^2). The LED strip was positioned around the external surface of the reactor so the light source uniformly irradiated the reaction volume. The suspension was left in dark conditions for 2 h to reach the adsorption–desorption equilibrium of glycerol on the photocatalyst surface. The effect of catalyst dosage, initial glycerol concentration, solution pH, and incident light intensity was evaluated. Moreover, the stability of the optimized photocatalyst after four reuse cycles was also evaluated. The analysis of the H_2 in the gaseous phase coming from the photoreactor during the irradiation time was performed by using a continuous analyzer (ABB Advance Optima AO2020) equipped with a thermal conductivity detector (TCD).

3. Results and Discussion

3.1. Photocatalytic Activity Tests

3.1.1. Influence of Cu Content on the Hydrogen Production under Visible Light

The photocatalytic hydrogen production was evaluated for undoped ZnO and Cu-doped ZnO photocatalysts under visible light from a glycerol aqueous solution at 5 wt % initial concentration and with a catalyst dosage equal to 1.5 g/L. Figure 1 reports the results obtained after 4 h of visible light irradiation. It is worthwhile to note that the hydrogen production obtained with undoped ZnO (612 µmol/L) was comparable to that obtained by photolysis alone (592 µmol/L). This result means that the undoped ZnO was not active in the presence of visible light for the hydrogen production due to its large band gap energy [46]. On the other hand, all of the Cu-doped ZnO samples showed positive results towards hydrogen production under visible light irradiation. In detail, from the data presented in Figure 1, it is possible to observe that the hydrogen production increased with the increase of Cu content up to 1.08 mol %, but a further increase of the dopant level resulted in a decrease of photocatalytic hydrogen production.

In particular, the 1.08Cu_ZnO photocatalyst showed a hydrogen production equal to 4180 µmol/L. Possibly, the improved photocatalytic performances observed up to 1.08 mol % Cu content were due to the inhibition of the recombination rate of the electron–hole pairs [47]. However, the increase in Cu content beyond the optimal value induced a worsening of photocatalytic performances, indicating that an excess of dopant content may act as a recombination center of the electron gap pairs, as reported in previous works [37,48,49]. Regarding the comparison with the available literature data, it should be pointed out that in many cases, besides glycerol, in the solution there is the presence of a further sacrificial agent such as methanol or the addition of noble metals, which act as cocatalysts for hydrogen production [23]. A hydrogen production of 2600 µmol/L is reported starting from a glycerol solution with 6 wt % initial concentration and using a Pt/TiO_2 photocatalyst [15]. In particular, the hydrogen production reported in [15] was lower than that achieved with the 1.08Cu_ZnO catalyst, which showed good efficiency under visible light and in the absence of noble metals, allowing it to achieve a hydrogen production equal to twice that found in the literature.

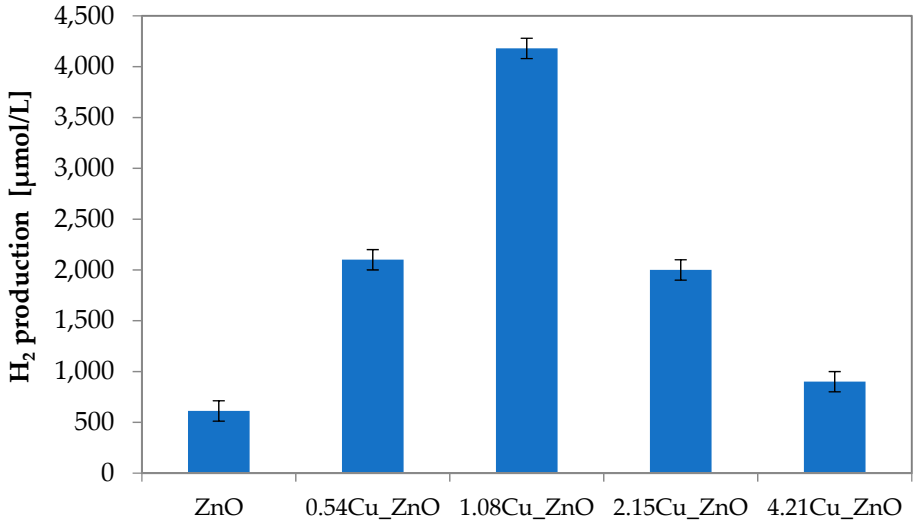

Figure 1. Influence of Cu content on hydrogen production under visible light after 4 h of visible irradiation time. Glycerol initial concentration: 5 wt %; catalyst dosage: 1.5 g/L; solution pH: 6; visible light intensity: 32 mW/cm^2.

It is well known that the parameter that defines the ability of a photocatalyst in hydrogen production is the electronic structure [50]. Considering that the copper content in the 1.08Cu_ZnO photocatalyst was very low (1.2 mol %), it is possible to assume its electronegativity value was equal to that of the undoped ZnO (5.94 eV) [46]. From the band gap value (E_g) of 1.08Cu_ZnO (2.92 eV), it was possible to calculate the values of conduction band (E_{CB}) and valence band (E_{VB}) energy through the Mulliken relationship [51]:

$$E_{VB} = X - 4.5 + (0.5 \times E_g)$$

$$E_{CB} = E_{VB} - E_g$$

where X is the semiconductor electronegativity.

The obtained results are presented in Figure 2.

As it is possible to observe from the E_{CB} (−0.05 eV vs. NHE) and E_{VB} (2.86 eV vs. NHE) values, the electronic structure of the 1.08Cu_ZnO photocatalyst satisfied the thermodynamic requirements for the water splitting reactions, with respect to the potentials for water oxidation/reduction reactions, reported also by Yerga et al. [52]. In fact, the E_{VB} value was equal to 2.89 eV versus NHE, which was more positive than the oxidation potential O_2/H_2O (+1.23 eV vs. NHE), and the E_{CB} value was equal to −0.05 eV versus NHE, which was more negative than the reduction potential H^+/H_2 (0 eV). Therefore, these values made the 1.08Cu_ZnO catalyst able to produce hydrogen in the presence of visible light both from thermodynamic and kinetic points of view thanks to the presence of the metal dopant that inhibited the recombination rate of the electron–hole pairs.

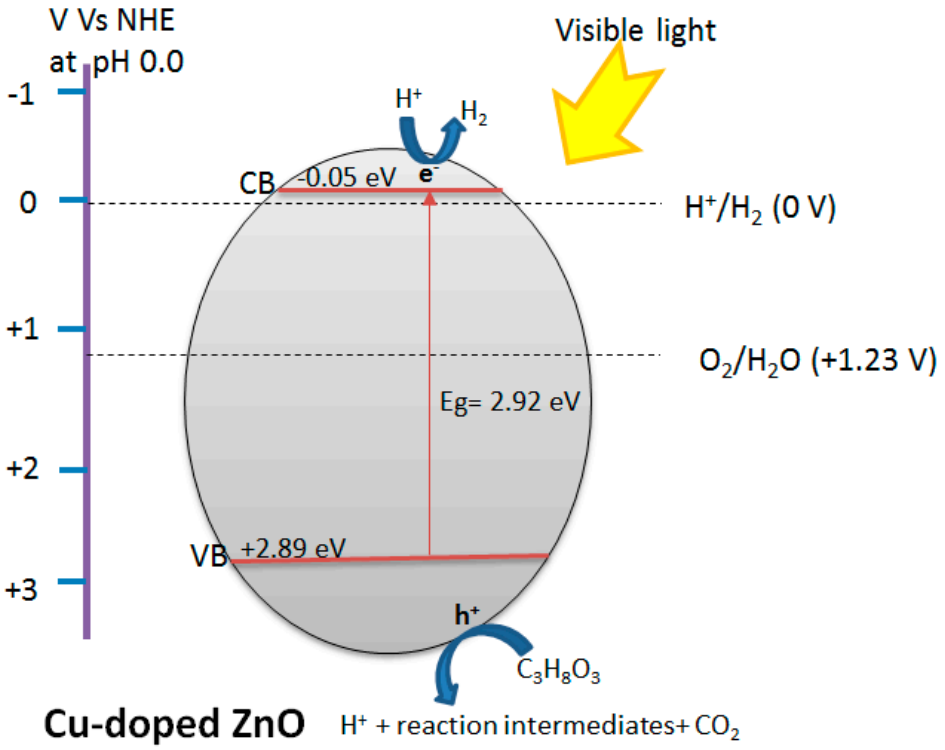

Figure 2. Proposed reaction mechanism for H_2 production from a glycerol aqueous solution using Cu-doped ZnO under visible light (CB: conduction band; VB: valence band).

3.1.2. Influence of 1.08Cu_ZnO Catalyst Dosage in Photocatalytic Hydrogen Production

The optimization of the photocatalyst dosage was obtained by testing different amounts of 1.08Cu_ZnO in the range of 0.75–3 g/L (Figure 3).

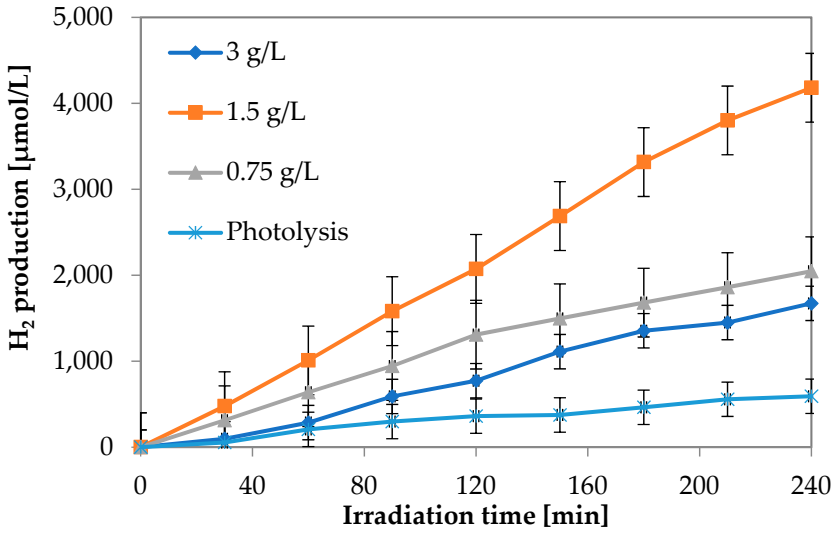

Figure 3. Hydrogen production during the irradiation time as a function of catalyst dosage. Glycerol initial concentration: 5 wt %; solution pH: 6; visible light intensity: 32 mW/cm^2; photocatalyst: 1.08Cu_ZnO.

Figure 3 displays the hydrogen production for the different 1.08Cu_ZnO dosages as a function of visible light irradiation time. As expected, very low H_2 production was observed for the photolysis test (without the photocatalyst). In the opposite way, the photocatalytic H_2 production from the glycerol

solution was significantly enhanced in the presence of the 1.08Cu_ZnO photocatalyst in the glycerol aqueous solution. At a fixed irradiation time, there was an increase of hydrogen production up to a 1.08Cu_ZnO dosage of 1.5 g/L (4180 µmol/L of H_2 after 4 h of visible light irradiation). Beyond this value of catalyst dosage, the photocatalytic performances worsened. In particular, at 3 g/L of catalyst dosage, the hydrogen production was 1670 µmol/L lower than that obtained with 0.75 g/L of catalyst dosage. The worsening of photocatalytic activity may be explained by the increased opacity of the aqueous solution, which made light penetration through the solution increasingly difficult [53]. Therefore, the optimal catalyst dosage was 1.5 g/L and it was used to evaluate the influence of the initial glycerol concentration in aqueous solution and the effect of pH of solution.

3.1.3. Effect of the Glycerol Initial Concentration on Photocatalytic Hydrogen Production

Figure 4 reports the effect of glycerol concentration on the amount of hydrogen produced during 4 h of visible irradiation time.

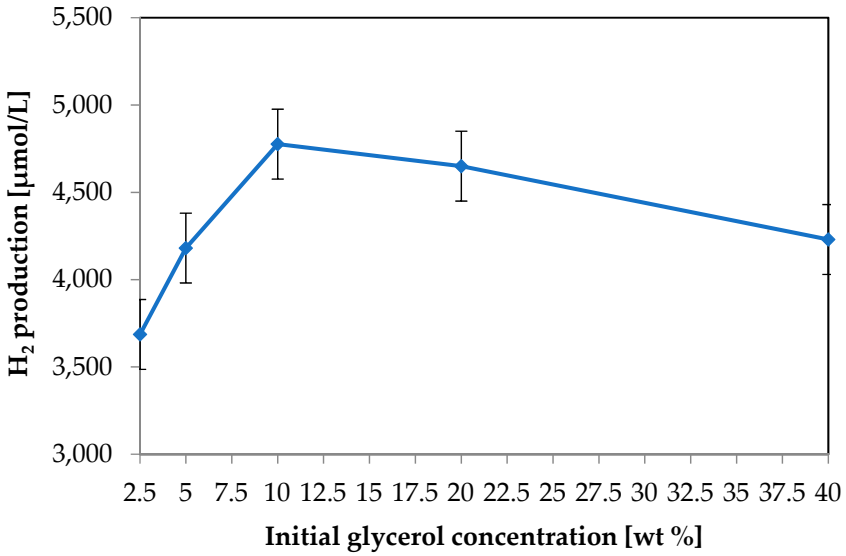

Figure 4. Photocatalytic hydrogen production during the irradiation time at different initial glycerol concentrations. Catalyst dosage: 1.5 g/L; solution pH: 6; visible light intensity: 32 mW/cm^2; photocatalyst: 1.08Cu_ZnO.

The results showed that hydrogen production increased with the increase of the glycerol concentration up to 10 wt % and then decreased for 20 and 40 wt % of glycerol initial concentration. Thus, the optimum glycerol concentration is to be considered equal to 10 wt %, with hydrogen production of 4776 µmol/L, as reported. The effect of the sacrificial agent initial concentration for photocatalytic hydrogen production has been extensively discussed in the literature. In particular, some studies have evidenced that this behavior follows a Langmuir-type isotherm [54–56], meaning that the photocatalytic hydrogen production rate is controlled by saturation of active centers by the adsorbed glycerol molecules [32]. However, in the present study, the interpretation of the data through a Langmuir-type isotherm does not adapt to the obtained experimental results; rather, the results show the existence of an optimum glycerol concentration. The worsening of the photocatalytic activity beyond the optimal value of the initial glycerol concentration can be attributed to the blockage of the adsorption of H_3O+ on the active site's surface [32]. Moreover, the existence of a maximum value for hydrogen production as a function of initial glycerol concentration could be also attributed to the action of glycerol as a quenching agent for ions and radicals generated during the irradiation [18].

3.1.4. Effect of pH on Photocatalytic Hydrogen Production

The effect of initial pH on H_2 photocatalytic production was evaluated in the range of 2–10 using the 1.08Cu_ZnO photocatalyst (Figure 5) with a glycerol initial concentration equal to 10 wt %.

The highest H_2 production was obtained at pH equal to 6 (H_2 production equal to 4776 µmol/L). It was evident that the change in pH had in any case worsened the overall production of hydrogen, which in acidic conditions was equal to 2771 µmol/L and in basic conditions was only 1764 µmol/L. Therefore, the best result was obtained by operating at the spontaneous pH of the glycerol aqueous solution (pH = 6). This can be seen as an advantage, particularly from an economic point of view, since it is not necessary to use additional chemicals to change the pH in order to improve the production of hydrogen. The increase of hydrogen production observed with the increase of initial pH from 2 up to 6 was consistent with the literature concerning glycerol photoreforming [17]. The best hydrogen evolution rate could be related to the adsorption of glycerol on the photocatalyst surface [17,18], the charging behavior of the semiconductor surface, the size of the aggregates of the photocatalyst particles, as well as the positions of the valence and conduction band levels of the semiconductor with respect to those of the redox couples in solution [57].

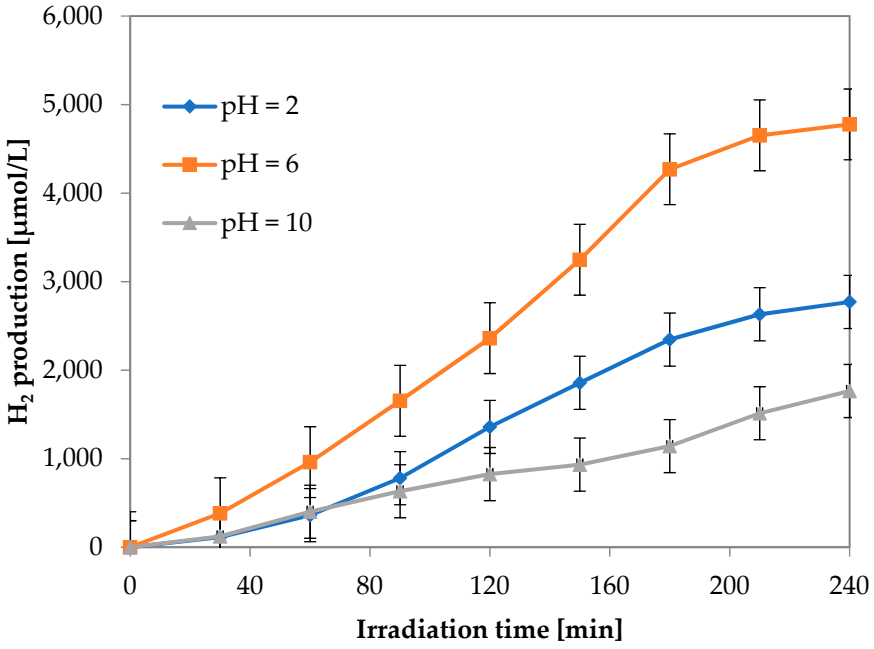

Figure 5. Photocatalytic hydrogen production during the irradiation time at different initial pH levels of solution. Glycerol initial concentration: 10 wt %; catalyst dosage: 1.5 g/L; visible light intensity: 32 mW/cm^2; photocatalyst: 1.08Cu_ZnO.

3.1.5. Influence of Visible Light Intensity on Photocatalytic Hydrogen Production

The influence of visible light intensity on photocatalytic hydrogen production was studied with an initial glycerol concentration equal to 10 wt % at the spontaneous pH of the solution and with the 1.08Cu_ZnO catalyst dosage equal to 1.5 g/L. In particular, the incident light intensity increased from 8 to 32 mW/cm^2. The obtained results are displayed in Figure 6.

As expected, at a fixed irradiation time, photocatalytic hydrogen production increased as LED light intensity increased due to the photogeneration of more electrons and holes [58]. These results are in agreement with the literature data that highlight the effect of light intensity on the performances of photocatalytic processes [59,60].

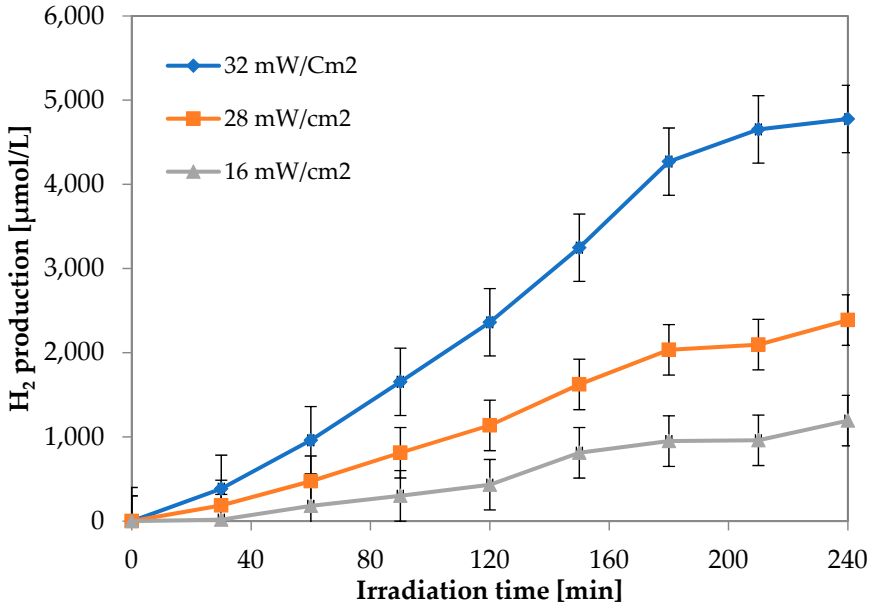

Figure 6. Photocatalytic hydrogen production for different visible light intensities. Initial glycerol concentration: 10 wt %; catalyst dosage: 1.5 g/L.

3.1.6. Recyclability Tests

Recyclability is one of the most important aspects to be considered in the formulation of a photocatalyst [59,61]. To confirm the recyclability of the 1.08Cu_ZnO sample, the photocatalytic tests for hydrogen production were repeated up to four cycles (Figure 7). At the end of each test, the catalyst was recovered by centrifugation of the solution, it was dried at room temperature for 48 h, and any regeneration step was carried out on the recovered catalyst.

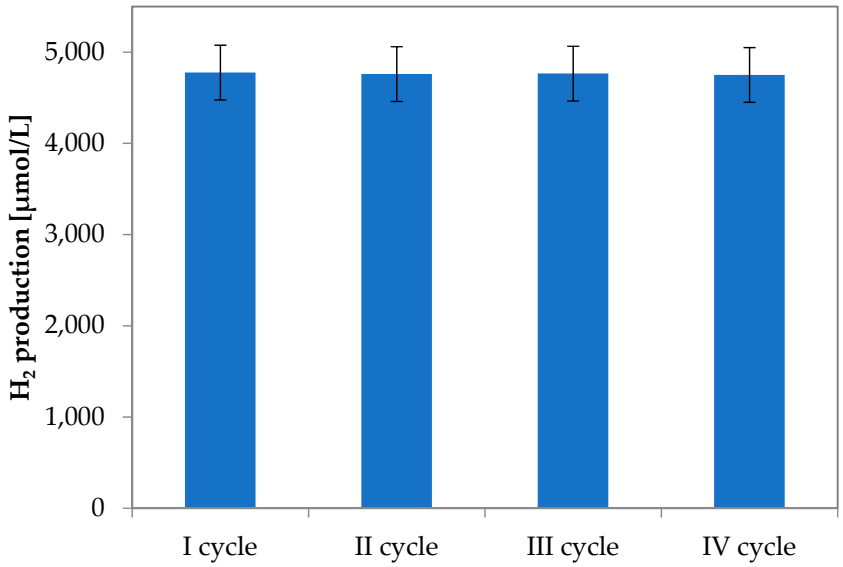

Figure 7. Evaluation of hydrogen production after 4 h of irradiation on the 1.08Cu_ZnO catalyst for different cycles. Initial glycerol concentration 10 wt %; UV light intensity: 32 mW/cm^2.

For all the reuse cycles, photocatalytic hydrogen production was substantially unchanged, being in the range of 4750–4775 µmol/L. These results evidenced the stability of the Cu-doped ZnO sample in photocatalytic hydrogen production from a glycerol aqueous solution under visible light and that

no photocorrosion phenomena (typical of ZnO-based photocatalysts [62–64]) occurred in the used operating conditions.

4. Conclusions

Cu-doped ZnO-based photocatalysts, prepared by a precipitation method, were studied in photocatalytic hydrogen production under visible light from a glycerol aqueous solution. The influence of the Cu content and operating conditions (initial glycerol concentration, photocatalyst dosage, light intensity, and initial pH of solution) were assessed. The highest hydrogen production was obtained at an optimum Cu content of 1.08 mol % with 10 wt % glycerol concentration, at the spontaneous pH of the solution (pH = 6), and with a photocatalyst dosage of 1.5 g/L. The electron transfer paths, induced by visible light irradiation, underlined that the 1.08Cu_ZnO catalyst is able to produce hydrogen in the presence of visible light both from thermodynamic and kinetic points of view since the doping with Cu inhibits the recombination rate of the photogenerated electron–hole pairs. Moreover, the optimized photocatalyst has proved to be active for several reuse cycles, maintaining the same hydrogen production and evidencing the absence of photocorrosion phenomena in the optimized operating conditions.

Supplementary Materials: The following are available online at http://www.mdpi.com/2076-3417/9/13/2741/s1.

Author Contributions: G.I. performed the experiments and wrote the manuscript. V.V. provided the concept and experimental design of the study and reviewed the paper prior to submission. Both the authors discussed the results, analyzed the data, and commented on the manuscript.

Funding: This research received no external funding.

Acknowledgments: The authors wish to thank Eng. Valentina Cirino for the help in the experimental tests.

Conflicts of Interest: The authors declare no conflict of interests.

References

1. Chang, C.-J.; Lin, Y.-G.; Weng, H.-T.; Wei, Y.-H. Photocatalytic hydrogen production from glycerol solution at room temperature by zno-zns/graphene photocatalysts. *Appl. Surf. Sci.* **2018**, *451*, 198–206. [CrossRef]
2. Halabi, M.; De Croon, M.; Van der Schaaf, J.; Cobden, P.; Schouten, J. Low temperature catalytic methane steam reforming over ceria–zirconia supported rhodium. *Appl. Catal. A Gen.* **2010**, *389*, 68–79. [CrossRef]
3. Li, Q.; Guo, B.; Yu, J.; Ran, J.; Zhang, B.; Yan, H.; Gong, J.R. Highly efficient visible-light-driven photocatalytic hydrogen production of cds-cluster-decorated graphene nanosheets. *J. Am. Chem. Soc.* **2011**, *133*, 10878–10884. [CrossRef] [PubMed]
4. Kim, J.; Park, Y.; Park, H. Solar hydrogen production coupled with the degradation of a dye pollutant using TiO_2 modified with platinum and nafion. *Int. J. Photoenergy* **2014**, *2014*, 324859. [CrossRef]
5. Maeda, K.; Teramura, K.; Lu, D.; Takata, T.; Saito, N.; Inoue, Y.; Domen, K. Photocatalyst releasing hydrogen from water. *Nature* **2006**, *440*, 295. [CrossRef] [PubMed]
6. Kudo, A.; Miseki, Y. Heterogeneous photocatalyst materials for water splitting. *Chem. Soc. Rev.* **2009**, *38*, 253–278. [CrossRef] [PubMed]
7. Chen, X.; Lou, Y.; Dayal, S.; Qiu, X.; Krolicki, R.; Burda, C.; Zhao, C.; Becker, J. Doped semiconductor nanomaterials. *J. Nanosci. Nanotechnol.* **2005**, *5*, 1408–1420. [CrossRef]
8. Gallo, A.; Montini, T.; Marelli, M.; Minguzzi, A.; Gombac, V.; Psaro, R.; Fornasiero, P.; Dal Santo, V. H2 production by renewables photoreforming on Pt–Au/TiO_2 catalysts activated by reduction. *ChemSusChem* **2012**, *5*, 1800–1811. [CrossRef]
9. Selli, E.; Chiarello, G.L.; Quartarone, E.; Mustarelli, P.; Rossetti, I.; Forni, L. A photocatalytic water splitting device for separate hydrogen and oxygen evolution. *Chem. Commun.* **2007**, *21*, 5022–5024. [CrossRef]
10. Iervolino, G.; Vaiano, V.; Sannino, D.; Rizzo, L.; Galluzzi, A.; Polichetti, M.; Pepe, G.; Campiglia, P. Hydrogen production from glucose degradation in water and wastewater treated by Ru-$LaFeO_3$/Fe_2O_3 magnetic particles photocatalysis and heterogeneous photo-fenton. *Int. J. Hydrogen Energy* **2018**, *43*, 2184–2196. [CrossRef]

11. Lucchetti, R.; Onotri, L.; Clarizia, L.; Di Natale, F.; Di Somma, I.; Andreozzi, R.; Marotta, R. Removal of nitrate and simultaneous hydrogen generation through photocatalytic reforming of glycerol over "in situ" prepared zero-valent nano copper/P25. *Appl. Catal. B Environ.* **2017**, *202*, 539–549. [CrossRef]
12. Christoforidis, K.C.; Fornasiero, P. Photocatalytic hydrogen production: A rift into the future energy supply. *ChemCatChem* **2017**, *9*, 1523–1544. [CrossRef]
13. Kawai, T.; Sakata, T. Photocatalytic hydrogen production from liquid methanol and water. *J. Chem. Soc. Chem. Commun.* **1980**, *15*, 694–695. [CrossRef]
14. Sakata, T.; Kawai, T. Heterogeneous photocatalytic production of hydrogen and methane from ethanol and water. *Chem. Phys. Lett.* **1981**, *80*, 341–344. [CrossRef]
15. Kondarides, D.I.; Daskalaki, V.M.; Patsoura, A.; Verykios, X.E. Hydrogen production by photo-induced reforming of biomass components and derivatives at ambient conditions. *Catal. Lett.* **2008**, *122*, 26–32. [CrossRef]
16. Harada, H.; Sakata, T.; Ueda, T. Effect of semiconductor on photocatalytic decomposition of lactic acid. *J. Am. Chem. Soc.* **1985**, *107*, 1773–1774. [CrossRef]
17. Li, M.; Li, Y.; Peng, S.; Lu, G.; Li, S. Photocatalytic hydrogen generation using glycerol wastewater over pt/tio 2. *Front. Chem. China* **2009**, *4*, 32–38. [CrossRef]
18. Vaiano, V.; Lara, M.A.; Iervolino, G.; Matarangolo, M.; Navio, J.A.; Hidalgo, M.C. Photocatalytic H2 production from glycerol aqueous solutions over fluorinated Pt-TiO_2 with high {001} facet exposure. *J. Photochem. Photobiol. A Chem.* **2018**, *365*, 52–59. [CrossRef]
19. Pradima, J.; Kulkarni, M.R. Review on enzymatic synthesis of value added products of glycerol, a by-product derived from biodiesel production. *Resour.-Eff. Technol.* **2017**, *3*, 394–405. [CrossRef]
20. Lalitha, K.; Sadanandam, G.; Kumari, V.D.; Subrahmanyam, M.; Sreedhar, B.; Hebalkar, N.Y. Highly stabilized and finely dispersed Cu2o/TiO_2: A promising visible sensitive photocatalyst for continuous production of hydrogen from glycerol: Water mixtures. *J. Phys. Chem. C* **2010**, *114*, 22181–22189. [CrossRef]
21. Montini, T.; Gombac, V.; Sordelli, L.; Delgado, J.J.; Chen, X.; Adami, G.; Fornasiero, P. Nanostructured Cu/TiO_2 photocatalysts for H_2 production from ethanol and glycerol aqueous solutions. *ChemCatChem* **2011**, *3*, 574–577. [CrossRef]
22. Lv, R.; Wang, X.; Lv, W.; Xu, Y.; Ge, Y.; He, H.; Li, G.; Wu, X.; Li, X.; Li, Q. Facile synthesis of ZnO nanorods grown on graphene sheets and its enhanced photocatalytic efficiency. *J. Chem. Technol. Biotechnol.* **2015**, *90*, 550–558. [CrossRef]
23. Jung, M.; Hart, J.N.; Boensch, D.; Scott, J.; Ng, Y.H.; Amal, R. Hydrogen evolution via glycerol photoreforming over Cu–Pt nanoalloys on TiO_2. *Appl. Catal. A Gen.* **2016**, *518*, 221–230. [CrossRef]
24. Patsoura, A.; Kondarides, D.I.; Verykios, X.E. Photocatalytic degradation of organic pollutants with simultaneous production of hydrogen. *Catal. Today* **2007**, *124*, 94–102. [CrossRef]
25. Wang, C.; Cai, X.; Chen, Y.; Cheng, Z.; Luo, X.; Mo, S.; Jia, L.; Shu, R.; Lin, P.; Yang, Z. Efficient hydrogen production from glycerol photoreforming over Ag_2OTiO_2 synthesized by a sol–gel method. *Int. J. Hydrogen Energy* **2017**, *42*, 17063–17074. [CrossRef]
26. Tanaka, A.; Hashimoto, K.; Kominami, H. Visible-light-induced hydrogen and oxygen formation over Pt/Au/Wo_3 photocatalyst utilizing two types of photoabsorption due to surface plasmon resonance and band-gap excitation. *J. Am. Chem. Soc.* **2014**, *136*, 586–589. [CrossRef] [PubMed]
27. Wang, P.; Huang, B.; Qin, X.; Zhang, X.; Dai, Y.; Wei, J.; Whangbo, M.H. Ag@AgCl: A highly efficient and stable photocatalyst active under visible light. *Angew. Chem. Int. Ed.* **2008**, *47*, 7931–7933. [CrossRef] [PubMed]
28. Yan, H.; Yang, J.; Ma, G.; Wu, G.; Zong, X.; Lei, Z.; Shi, J.; Li, C. Visible-light-driven hydrogen production with extremely high quantum efficiency on Pt–Pds/CdS photocatalyst. *J. Catal.* **2009**, *266*, 165–168. [CrossRef]
29. Anker, J.N.; Hall, W.P.; Lyandres, O.; Shah, N.C.; Zhao, J.; Van Duyne, R.P. Biosensing with plasmonic nanosensors. In *Nanoscience and Technology: A Collection of Reviews from Nature Journals*; World Scientific: Singapore, 2010; pp. 308–319.
30. Slamet, S.; Kusrini, E.; Afrozi, A.; Ibadurrohman, M. Photocatalytic hydrogen production from glycerol-water over metal loaded and non-metal doped titanium oxide. *Int. J. Technol.* **2015**, *6*, 520–532. [CrossRef]
31. Kanade, K.; Kale, B.; Baeg, J.-O.; Lee, S.M.; Lee, C.W.; Moon, S.-J.; Chang, H. Self-assembled aligned Cu doped ZnO nanoparticles for photocatalytic hydrogen production under visible light irradiation. *Mater. Chem. Phys.* **2007**, *102*, 98–104. [CrossRef]

32. Tristantini, D.; Ibadurrohman, M. Photocatalytic hydrogen production from glycerol-water mixture over Pt-N-TiO_2 nanotube photocatalyst. *Int. J. Energy Res.* **2013**, *37*, 1372–1381.
33. Kum, J.M.; Park, Y.J.; Kim, H.J.; Cho, S.O. Plasmon-enhanced photocatalytic hydrogen production over visible-light responsive Cu/TiO_2. *Nanotechnology* **2015**, *26*, 125402. [CrossRef] [PubMed]
34. Clarizia, L.; Spasiano, D.; Di Somma, I.; Marotta, R.; Andreozzi, R.; Dionysiou, D.D. Copper modified-TiO_2 catalysts for hydrogen generation through photoreforming of organics. A short review. *Int. J. Hydrogen Energy* **2014**, *39*, 16812–16831. [CrossRef]
35. Yu, Z.; Meng, J.; Li, Y.; Li, Y. Efficient photocatalytic hydrogen production from water over a CuO and carbon fiber comodified TiO_2 nanocomposite photocatalyst. *Int. J. Hydrogen Energy* **2013**, *38*, 16649–16655. [CrossRef]
36. Goyal, P.; Chakraborty, S.; Misra, S.K. Multifunctional Fe_3O_4-ZnO nanocomposites for environmental remediation applications. *Environ. Nanotechnol. Monit. Manag.* **2018**, *10*, 28–35. [CrossRef]
37. Vaiano, V.; Iervolino, G.; Rizzo, L. Cu-doped ZnO as efficient photocatalyst for the oxidation of arsenite to arsenate under visible light. *Appl. Catal. B Environ.* **2018**, *238*, 471–479. [CrossRef]
38. Vaiano, V.; Iervolino, G. Facile method to immobilize ZnO particles on glass spheres for the photocatalytic treatment of tannery wastewater. *J. Colloid Interface sci.* **2018**, *518*, 192–199. [CrossRef] [PubMed]
39. Lee, K.M.; Lai, C.W.; Ngai, K.S.; Juan, J.C. Recent developments of zinc oxide based photocatalyst in water treatment technology: A review. *Water Res.* **2016**, *88*, 428–448. [CrossRef]
40. Mohan, R.; Krishnamoorthy, K.; Kim, S.-J. Enhanced photocatalytic activity of Cu-doped ZnO nanorods. *Solid State Commun.* **2012**, *152*, 375–380. [CrossRef]
41. Shirzad-Siboni, M.; Jonidi-Jafari, A.; Farzadkia, M.; Esrafili, A.; Gholami, M. Enhancement of photocatalytic activity of Cu-doped ZnO nanorods for the degradation of an insecticide: Kinetics and reaction pathways. *J. Environ. Manag.* **2017**, *186*, 1–11. [CrossRef]
42. Ma, H.; Yue, L.; Yu, C.; Dong, X.; Zhang, X.; Xue, M.; Zhang, X.; Fu, Y. Synthesis, characterization and photocatalytic activity of Cu-doped Zn/ZnO photocatalyst with carbon modification. *J. Mater. Chem.* **2012**, *22*, 23780–23788. [CrossRef]
43. Mittal, M.; Sharma, M.; Pandey, O. UV–visible light induced photocatalytic studies of Cu doped ZnO nanoparticles prepared by co-precipitation method. *Sol. Energy* **2014**, *110*, 386–397. [CrossRef]
44. Wang, M.; Ren, F.; Cai, G.; Liu, Y.; Shen, S.; Guo, L. Activating ZnO nanorod photoanodes in visible light by cu ion implantation. *Nano Res.* **2014**, *7*, 353–364. [CrossRef]
45. Sharma, P.K.; Kumar, M.; Pandey, A.C. Green luminescent zno: Cu^{2+} nanoparticles for their applications in white-light generation from uv leds. *J. Nanopart. Res.* **2011**, *13*, 1629–1637. [CrossRef]
46. Martha, S.; Reddy, K.H.; Parida, K. Fabrication of In_2O_3 modified ZnO for enhancing stability, optical behaviour, electronic properties and photocatalytic activity for hydrogen production under visible light. *J. Mater. Chem. A* **2014**, *2*, 3621–3631. [CrossRef]
47. Kadam, A.; Kim, T.G.; Shin, D.S.; Garadkar, K.; Park, J. Morphological evolution of Cu doped ZnO for enhancement of photocatalytic activity. *J. Alloys Compd.* **2017**, *710*, 102–113. [CrossRef]
48. Ola, O.; Maroto-Valer, M.M. Review of material design and reactor engineering on TiO_2 photocatalysis for CO_2 reduction. *J. Photochem. Photobiol. C Photochem. Rev.* **2015**, *24*, 16–42. [CrossRef]
49. Chen, P. A promising strategy to fabricate the Cu/$BiVO_4$ photocatalysts and their enhanced visible-light-driven photocatalytic activities. *J. Mater. Sci. Mater. Electron.* **2016**, *27*, 2394–2403. [CrossRef]
50. Yerga, R.M.N.; Alvarez-Galvan, M.C.; Vaquero, F.; Arenales, J.; Fierro, J.L.G. Hydrogen production from water splitting using photo-semiconductor catalysts. In *Renewable Hydrogen Technologies*; Elsevier: Amsterdam, The Netherlands, 2013; pp. 43–61.
51. Nenavathu, B.P.; Kandula, S.; Verma, S. Visible-light-driven photocatalytic degradation of safranin-t dye using functionalized graphene oxide nanosheet (fgs)/Zno nanocomposites. *RSC Adv.* **2018**, *8*, 19659–19667. [CrossRef]
52. Navarro Yerga, R.M.; Alvarez Galvan, M.C.; Del Valle, F.; Villoria de la Mano, J.A.; Fierro, J.L. Water splitting on semiconductor catalysts under visible-light irradiation. *ChemSusChem Chem. Sustain. Energy Mater.* **2009**, *2*, 471–485. [CrossRef]
53. Vaiano, V.; Iervolino, G.; Sannino, D.; Rizzo, L.; Sarno, G.; Farina, A. Enhanced photocatalytic oxidation of arsenite to arsenate in water solutions by a new catalyst based on moox supported on TiO_2. *Appl. Catal. B Environ.* **2014**, *160*, 247–253. [CrossRef]

54. Li, Y.; Lu, G.; Li, S. Photocatalytic hydrogen generation and decomposition of oxalic acid over platinized TiO_2. *Appl. Catal. A Gen.* **2001**, *214*, 179–185. [CrossRef]
55. Wei, L.F.; Zheng, X.J.; Zhang, Z.H.; Wei, Y.J.; Xie, B.; Wei, M.B.; Sun, X.L. A systematic study of photocatalytic H_2 production from propionic acid solution over Pt/TiO_2 photocatalyst. *Int. J. Energy Res.* **2012**, *36*, 75–86. [CrossRef]
56. Strataki, N.; Bekiari, V.; Kondarides, D.I.; Lianos, P. Hydrogen production by photocatalytic alcohol reforming employing highly efficient nanocrystalline titania films. *Appl. Catal. B Environ.* **2007**, *77*, 184–189. [CrossRef]
57. Daskalaki, V.M.; Kondarides, D.I. Efficient production of hydrogen by photo-induced reforming of glycerol at ambient conditions. *Catal. Today* **2009**, *144*, 75–80. [CrossRef]
58. Tambago, H.M.G.; de Leon, R.L. Intrinsic kinetic modeling of hydrogen production by photocatalytic water splitting using cadmium zinc sulfide catalyst. *Int. J. Chem. Eng. Appl.* **2015**, *6*, 220–227. [CrossRef]
59. Vaiano, V.; Iervolino, G.; Sannino, D.; Rizzo, L.; Sarno, G. $MoOx/TiO_2$ immobilized on quartz support as structured catalyst for the photocatalytic oxidation of as (iii) to as (v) in aqueous soluTiOns. *Chem. Eng. Res. Des.* **2016**, *109*, 190–199. [CrossRef]
60. Sannino, D.; Vaiano, V.; Sacco, O.; Ciambelli, P. Mathematical modelling of photocatalytic degradation of methylene blue under visible light irradiation. *J. Environ. Chem. Eng.* **2013**, *1*, 56–60. [CrossRef]
61. Sorathiya, K.; Mishra, B.; Kalarikkal, A.; Reddy, K.P.; Gopinath, C.S.; Khushalani, D. Enhancement in rate of photocatalysis upon catalyst recycling. *Sci. Rep.* **2016**, *6*, 35075. [CrossRef]
62. Chen, Z.; Zhang, N.; Xu, Y.-J. Synthesis of graphene–zno nanorod nanocomposites with improved photoactivity and anti-photocorrosion. *CrystEngComm* **2013**, *15*, 3022–3030. [CrossRef]
63. Zhang, Y.; Chen, Z.; Liu, S.; Xu, Y.-J. Size effect induced activity enhancement and anti-photocorrosion of reduced graphene oxide/zno composites for degradation of organic dyes and reduction of Cr(VI) in water. *Appl. Catal. B Environ.* **2013**, *140–141*, 598–607. [CrossRef]
64. Ishioka, J.; Kogure, K.; Ofuji, K.; Kawaguchi, K.; Jeem, M.; Kato, T.; Shibayama, T.; Watanabe, S. In situ direct observation of photocorrosion in zno crystals in ionic liquid using a laser-equipped high-voltage electron microscope. *AIP Adv.* **2017**, *7*, 035220. [CrossRef]